MHD effects on natural convection laminar flow from a horizontal circular cylinder in presence of radiation

Tariq Javed, Abid Majeed and Irfan Mustafa*
Department of Mathematics and Statistics,
FBAS, International Islamic University, Islamabad 44000, Pakistan.
**Tel.: +92 51 9019511.*
e-mail: irfanmustafa1983@yahoo.com

Received 3 June 2015; accepted 14 September 2015

In this study, the effect of magnetohydrodynamic (MHD) on natural convection flow from a horizontal circular cylinder in the presence of radiation has been investigated. The governing boundary layer equations are converted into non-dimensional partial differential equations by using the suitable transformation and then solved numerically by employing an accurate implicit finite difference scheme known as Keller-box method. We presented the influence of emerging non-dimensional parameters namely the MHD parameter M with combination of surface heating parameter θ_w and radiation-conduction parameter R_d on velocity and temperature profiles, skin friction coefficient and Nusselt number through graphs and tables. It is observed that the Lorentz force reduces the velocity, skin friction coefficient and Nusselt number. Moreover temperature increases in the presence of MHD effect. The streamlines and isotherms reflect some attractive flow patterns which show that magnetic parameter M and radiation parameter R_d have deep influence on these fluid and heat flow patterns.

Keywords: MHD; radiation; horizontal circular cylinder; numerical solution.

PACS: 47.10.ad; 02.60.Cb; 44.20.+b

1. Introduction

Natural convection flow around a heated circular cylinder for different fluids has great importance owing to their wide applications in industries. The heat convection around cylindrical bodies has fascinated many researchers due to the fact that cylinders have been used in nuclear waste disposal, energy extortion in underground and catalytic beds. Natural convection driven by temperature difference has been examined in detail. Through literature survey it divulges that Merkin [1,2] was the first to initiate the free convection boundary layer flow on horizontal circular cylinders and cylinders with elliptic cross-section. Sparrow and Lee [3] considered the effects of mixed convection around a circular cylinder. In 1983, Luciano and Socio [4] investigated free convection around horizontal circular cylinders. They performed experiments to calculate average and local Nusselt numbers. Different characteristics of the flow regions were shown through visual observations. Merkin [5] studied free convection boundary layer flow on an isothermal horizontal circular cylinder. Ingham [6] examined free convection boundary layer flow on an isothermal horizontal cylinder. By considering the micro-polar fluid, Nazar *et al*. [7, 8] have discussed the natural convection flow along a uniformly heated horizontal circular cylinder and described the effects of micro-rotation of the fluid from lower to upper stagnation point after the work of Merkin [5] on isothermal circular cylinder. Molla *et al*. [9-11] studied the analysis of natural convection flow from an isothermal horizontal circular cylinder by considering temperature dependent viscosity, heat generation and uniform heat flux. Bhowmicket *et al*. [12] investigated natural convection flow of non-Newtonian fluid along a horizontal circular cylinder with uniform surface heat flux by using a modified power law viscosity model. The governing equations were solved numerically by using implicit finite difference scheme of marching order with double sweep technique. Later, Javed *et al*. [13] considered natural convection flow in an isosceles triangular cavity filled with porous medium due to uniform/non-uniform heated side walls in the presence of MHD effect.

The study of thermal radiation on free convection flow has achieved immense importance among the researchers due to various engineering applications. Such applications are power generation plants, re-entry of space vehicle and high speed flights. It is well known that radiation effects altered the temperature distribution in the laminar boundary layer. Resultantly, it has an effect on heat transfer at the wall. The consecutive treatment of convective radiative heat transfer is essential in such circumstances. The interaction between convection and thermal radiation over different surfaces can be found in refs [14-29]. The situations where MHD and thermal radiation effects on flow and rate of heat transfer are important in many fields like geophysical, geothermal and engineering processes and appliances. The examples are nuclear reactors, nuclear waste disposal, grain storage, migration of moisture contained in fibrous insulations through air, dispersion of chemical pollutants through water-saturated soil, etc. The present paper is the extension of the work of Molla *et al*. [24] including MHD effects. To the best of our knowledge, this work has not been addressed in the literature earlier. The emerging transformed nonlinear partial differential equations are solved by using a stable and efficient implicit finite difference scheme (Keller-box method [30]). The obtained solution is discussed through graphs and tables for different values of emerging parameters.

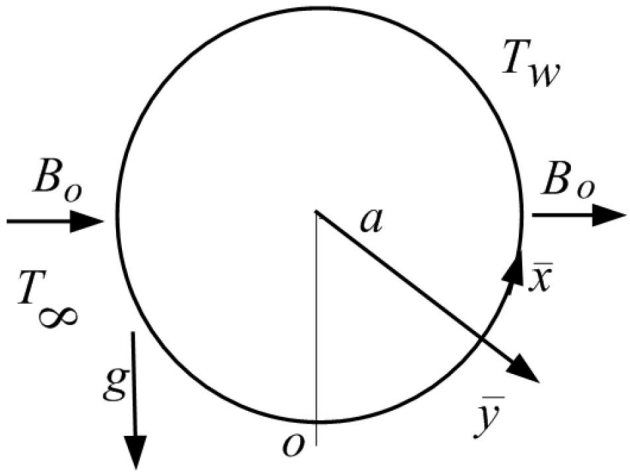

FIGURE 1. Geometry of the flow situation.

2. Mathematical formulation

Consider the free convection flow of two-dimensional steady incompressible viscous fluid over a circular cylinder of fixed radius a. A uniform magnetic field of strength B_0 along radial direction is applied perpendicular to the regular surface of cylinder. The $\bar{x}$ and $\bar{y}$ are coordinate measured along and perpendicular to the surface of the cylinder with origin at O as lower stagnation point ($\bar{x} \approx 0$). It is assumed that T_w and T_∞ are the surface temperature of the cylinder and ambient temperature of the fluid respectively. We have considered only the case $T_w > T_\infty$ corresponds to heated cylinder. The geometry of the flow situation is shown in Fig. 1. Following Merkin [5], the continuity and conservation equations will take the form as

$$\frac{\partial \bar{u}}{\partial \bar{x}} + \frac{\partial \bar{v}}{\partial \bar{y}} = 0 \tag{1}$$

$$\rho\left(\bar{u}\frac{\partial \bar{u}}{\partial \bar{x}} + \bar{v}\frac{\partial \bar{u}}{\partial \bar{y}}\right) = \mu\frac{\partial^2 \bar{u}}{\partial \bar{y}^2} + \rho g\beta(T - T_\infty)\sin\left(\frac{\bar{x}}{a}\right) - \sigma_0 B_0^2 \bar{u} \tag{2}$$

$$\bar{u}\frac{\partial T}{\partial \bar{x}} + \bar{v}\frac{\partial T}{\partial \bar{y}} = \frac{1}{\rho c_p}\frac{\partial}{\partial \bar{y}}\left[\left\{k + \frac{16\sigma T^3}{3(\alpha_r + \alpha_s)}\right\}\frac{\partial T}{\partial \bar{y}}\right] \tag{3}$$

where $\bar{u}$ and $\bar{v}$ be the velocity components along $\bar{x}$ and $\bar{y}$ directions respectively, T be the temperature of the fluid within the boundary layer, ρ and μ be the density and viscosity of the fluid respectively, g be the acceleration due to gravity, β be the coefficient of thermal expansion, B_0 be applied magnetic field acting normal at the cylinder surface, σ_0 be the electric conductivity of the fluid, c_p be the specific heat at constant pressure and σ be the Stephen-Boltzman constant, α_r and α_s are the Rosseland mean absorption coefficient and the scaling coefficient respectively. The radiation effect in Eq. (3) is considered by using the Rosseland diffusion approximation for radiation (Siegel and Howell [31]). Under this approximation the solution is not valid for situations where scattering is expected to be non-isotropic as well as in the immediate vicinity of the surface of the cylinder.

The related boundary conditions for the governing problem are

$$\left.\begin{array}{llll} \bar{u} = \bar{v} = 0, & T = T_w & \text{at} & \bar{y} = 0 \\ \bar{u} \to 0, & T \to T_\infty & \text{as} & \bar{y} \to \infty \end{array}\right\}. \tag{4}$$

The non-dimensional scaling variables are introduced as

$$\left.\begin{array}{llll} x = \dfrac{\bar{x}}{a}, & y = Gr^{\frac{1}{4}}\dfrac{\bar{y}}{a} & u = \dfrac{a}{v(nu)}Gr^{-\frac{1}{2}}\bar{u} & v = \dfrac{a}{v(nu)}Gr^{\frac{1}{4}}\bar{v} \\ \theta = \dfrac{T - T_\infty}{T_w - T_\infty}, & Gr = \dfrac{g\beta(T_w - T_\infty)a^3}{v^2} & & \end{array}\right\}. \tag{5}$$

where $\nu = \mu/\rho$ be the kinematic viscosity, Gr be the Grashof number and θ be the dimensionless temperature. Substituting non-dimensional scaling variables into Eqs. (1-3), we get the subsequent dimensionless partial differential equations.

$$\frac{\partial u}{\partial x} + \frac{\partial v}{\partial y} = 0 \tag{6}$$

$$u\frac{\partial u}{\partial x} + v\frac{\partial u}{\partial y} = \frac{\partial^2 u}{\partial y^2} + \theta\sin x - Mu, \tag{7}$$

$$u\frac{\partial \theta}{\partial x} + v\frac{\partial \theta}{\partial y} = \frac{1}{\text{Pr}} \times \frac{\partial}{\partial y}\left[\left\{1 + \frac{4}{3}R_d(1 + \Delta\theta)^3\right\}\frac{\partial \theta}{\partial y}\right] \tag{8}$$

with allied boundary conditions will become

$$\left.\begin{array}{llll} u = 0, & v = 0, & \theta = 1 \text{ at } y = 0 \\ u \to 0, & \theta \to 0, & \text{as } y \to \infty \end{array}\right\}, \tag{9}$$

where

$$\text{Pr} = \frac{\mu C_p}{k}, \quad R_d = \frac{4\sigma T_\infty^3}{k(\alpha_r + \alpha_s)}, \quad \theta_w = \frac{T_w}{T_\infty}, \quad \Delta = \theta_w - 1, \quad M = \frac{\sigma_0 a^2 B_0^2}{\mu Gr^{\frac{1}{2}}}, \tag{10}$$

where Pr be the Prandtl number, R_d be radiation-conduction parameter or Plank number, θ_w be the surface heating parameter and M be magnetic parameter. Equations (7, 8) with

boundary conditions (9) can be written in terms of stream function ψ defined in velocity component form as

$$u = \frac{\partial \psi}{\partial y}, \quad v = -\frac{\partial \psi}{\partial x} \tag{11}$$

Where

$$\psi = xf(x,y), \quad \theta = \theta(x,y) \tag{12}$$

Which identically satisfy the continuity Eq. (6). Upon using Eq. (11) into Eqs. (7,8), the transformed equations take the form

$$\frac{\partial^3 f}{\partial y^3} + f\frac{\partial^2 f}{\partial y^2} - \left(\frac{\partial f}{\partial y}\right)^2 + \frac{\sin x}{x}\theta - M\frac{\partial f}{\partial y} = x\left(\frac{\partial f}{\partial y}\frac{\partial^2 f}{\partial x \partial y} - \frac{\partial f}{\partial x}\frac{\partial^2 f}{\partial y^2}\right), \tag{13}$$

$$\frac{1}{\Pr}\frac{\partial}{\partial y}\left[\left\{1 + \frac{4}{3}R_d(1+(\theta_w-1)\theta)^3\right\}\frac{\partial \theta}{\partial y}\right] + f\frac{\partial \theta}{\partial y} = x\left(\frac{\partial f}{\partial y}\frac{\partial \theta}{\partial x} - \frac{\partial \theta}{\partial y}\frac{\partial f}{\partial x}\right), \tag{14}$$

with the boundary conditions

$$\left.\begin{array}{lll} f = \frac{\partial f}{\partial y} = 0, & \theta = 1 & \text{at } y = 0 \\ \frac{\partial f}{\partial y} \to 0, & \theta \to 0 & \text{as } y \to \infty \end{array}\right\} \tag{15}$$

For $x \approx 0$, the partial differential Eqs. (13, 14) take the following form

$$f''' + ff'' - f'^2 + \theta - Mf' = 0, \tag{16}$$

$$\frac{1}{\Pr}\left[\left\{1 + \frac{4}{3}R_d(1+(\theta_w-1)\theta)^3\right\}\theta'\right]' + f\theta' = 0 \tag{17}$$

and the boundary conditions (15) become

$$\left.\begin{array}{lll} f(0) = 0, & f'(0) = 0, & \theta(0) = 1 \\ f'(y) = 0, & \theta(y) = 0, & \text{as } y \to \infty \end{array}\right\} \tag{18}$$

For engineering point of view, the skin friction coefficient C_f and the local Nusselt number Nu, which are basically the quantities of interest are defined as

$$C_f = \frac{\tau_w}{\rho U_\infty^2} \quad and \quad Nu = \frac{aq_w}{k(T_w - T_\infty)}, \tag{19}$$

in which the shear stress and the heat flux at wall are

$$\tau_w = \mu\left(\frac{\partial \bar{u}}{\partial \bar{y}}\right)_{\bar{y}=0},$$

$$q_w = -\left[\left(\frac{16\sigma T^3}{3(\alpha_r + \alpha_s)} + k\right)\frac{\partial T}{\partial \bar{y}}\right]_{\bar{y}=0}. \tag{20}$$

Using the transformation (5), the skin friction coefficient ($C_f Gr^{1/4}$) and the local Nusselt number ($NuGr^{-1/4}$) can be written as

$$C_f Gr^{1/4} = x\frac{\partial^2 f(x,0)}{\partial y^2}, \tag{21}$$

$$NuGr^{-1/4} = -\left(1 + \frac{4}{3}R_d\theta_w^3\right)\frac{\partial \theta(x,0)}{\partial y}. \tag{22}$$

For the solution of nonlinear system of partial differential Eqs. (13, 14) subject to the boundary conditions (15), we employed an accurate and efficient implicit finite difference method commonly known as Keller box which is explained briefly in the next section while the details can be seen in the book of Cebeci and Bradshaw [30].

3. Numerical approach

A numerical solution of non-linear partial differential Eqs. (13) and (14) subject to the boundary conditions (15) is obtained by using implicit finite difference scheme known as Keller-box method. The following steps are followed to obtain the solution:

1. Reduce Eqs. (13) and (14) to a first order systems.
2. Convert them to difference equations by using central difference formula.
3. Linearize the resulting algebraic equations by using Newton's method and write them in matrix form.
4. Solve the obtained matrix form by using block-tridiagonal elimination technique.

The step sizes of Δx and Δy are in x and y respectively and edge of the boundary layer are adjusted for different range of parameters. The details of solution technique are not given due to limited space.

4. Result and Discussion

The governing non-dimensional partial differential Eqs. (13,14) subject to the boundary conditions (15) are solved by Keller Box scheme for some fixed values of Magnetic parameter M, Prandtl number Pr, Radiation parameter R_d and surface heating parameter θ_w. To verify our results, a comparison of numerical values of local Nusselt number and skin friction coefficient for $M = 0.0$, $R_d = 0.0$ as our limiting case with the results of Merkin [1], Nazar *et al.* [7] and Molla *et al.* [24] has been shown in Table I. The comparison of numerical results of skin friction coefficient $C_f Gr^{1/4}$ and that of Nusselt number $NuGr^{-1/4}$ have been shown against different numeric values of surface heating parameter θ_w in Table II & Table III being $R_d = 0.5$, Pr = 0.73 and $M = 0.0$ with Molla *et al.* [24]. It is observed that a good agreement

TABLE I. Comparison of $C_fGr^{1/4}$ and $NuGr^{-1/4}$ with those of Merkin [1], Nazar *et al.* [7] and Molla *et al.* [24], while Pr =1.0 and $R_d = 0$.

x	$C_fGr^{1/4}$				$NuGr^{-1/4}$			
	[1]	[7]	[24]	Present	[1]	[7]	[24]	Present
0	0.0000	0.0000	0.0000	0.0000	0.4214	0.4214	0.4216	0.4215
$\pi/6$	0.4151	0.4148	0.4139	0.4150	0.4161	0.4161	0.4163	0.4163
$\pi/3$	0.7558	0.7542	0.7527	0.7557	0.4007	0.4005	0.4006	0.4009
$\pi/2$	0.9579	0.9545	0.9526	0.9578	0.3745	0.3741	0.3741	0.3747
$2\pi/3$	0.9756	0.9698	0.9677	0.9555	0.3364	0.3355	0.3355	0.3364
$5\pi/6$	0.7822	0.7740	0.7717	0.7822	0.2825	0.2811	0.2810	0.2824
π	0.3391	0.3265	0.3238	0.3388	0.1945	0.1916	0.1911	0.1943

TABLE II. The comparison of $C_fGr^{1/4}$ for different values of θ_w while $R_d = 0.5$, $M = 0.0$ and Pr = 0.73.

x	$C_fGr^{1/4}$			
	$\theta_w = 1.1$		$\theta_w = 1.9$	
0	[24]	Present	[24]	Present
0	0.0000	0.0000	0.0000	0.0000
$\pi/6$	0.4700	0.4700	0.5202	0.5202
$\pi/3$	0.8476	0.8577	0.9511	0.9511
$\pi/2$	1.0920	1.0923	1.2158	1.2159
$2\pi/3$	1.1227	1.1232	1.2599	1.2602
$5\pi/6$	0.9218	0.9227	1.0543	1.0550
π	0.4572	0.4600	0.5729	0.5755

TABLE III. The comparison of $NuGr^{-1/4}$ for different values of θ_w while $R_d = 0.5$, $M = 0.0$ and Pr = 0.73.

x	$NuGr^{-1/4}$			
	$\theta_w = 1.1$		$\theta_w = 1.9$	
0	[24]	Present	[24]	Present
0	0.5436	0.5737	0.8572	0.8575
$\pi/6$	0.5376	0.5374	0.8478	0.8478
$\pi/3$	0.5187	0.5183	0.8186	0.8185
$\pi/2$	0.4864	0.4860	0.7693	0.7691
$2\pi/3$	0.4397	0.4394	0.6985	0.6984
$5\pi/6$	0.3750	0.3749	0.6022	0.6023
π	0.2762	0.2737	0.4634	0.4645

exists among these numerical values. Figures 2(a) and 2(b) present the variation in the velocity and temperature profiles against y for various values of radiation parameter R_d for both cases when $M = 0$ (absence of magnetic field) and $M = 0.5$ (in presence of magnetic field). It is found from Fig. 2(a) that increase in the radiation parameter provides the enhancement in fluid flow. Consequently, velocity profile is

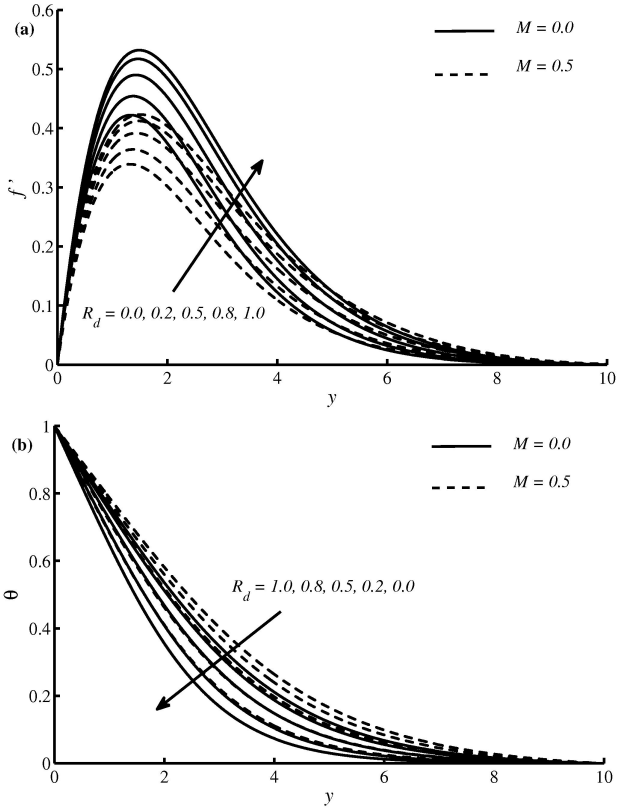

FIGURE 2. (a,b) Velocity and temperature profiles for different values of Rd while $\theta_w = 1.1$, Pr = 0.73 and $x = \pi/3$.

increased corresponding to increase values of R_d. On the other hand opposite behavior is observed in the presence of magnetic field $M = 0.5$. Physically, we can say that MHD provides the resistance in the fluid motion. Consequently, we can see that $M = 0.5$ shows low velocity profile as compare to $M = 0$ (absence of magnetic field). As concerned to the present study, we know that magnetic field produces electric current in fluid which produces heat in the fluid, so the magnetic field with radiation assists the heat production phenomena. The contribution of these effects can be visual-

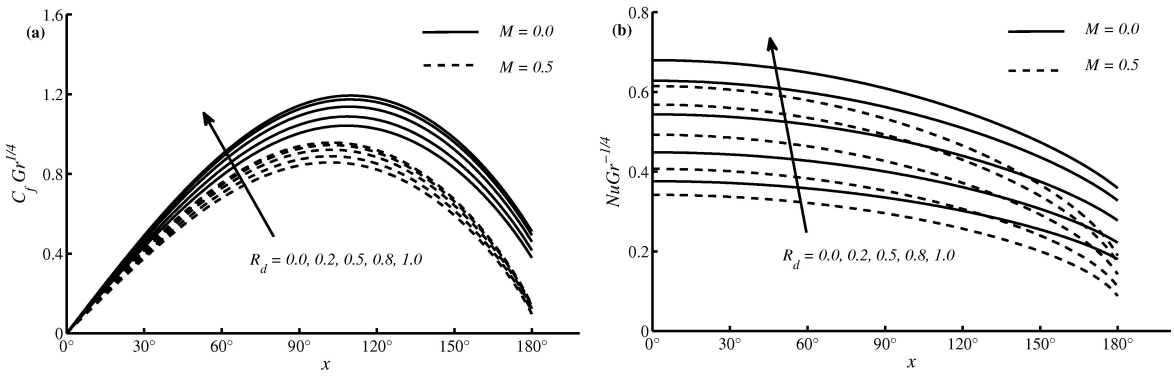

FIGURE 3. (a, b): Variation of $C_f Gr^{1/4}$ and $NuGr^{-1/4}$ for various values of R_d while $\theta_w = 1.1$ and Pr = 0.73.

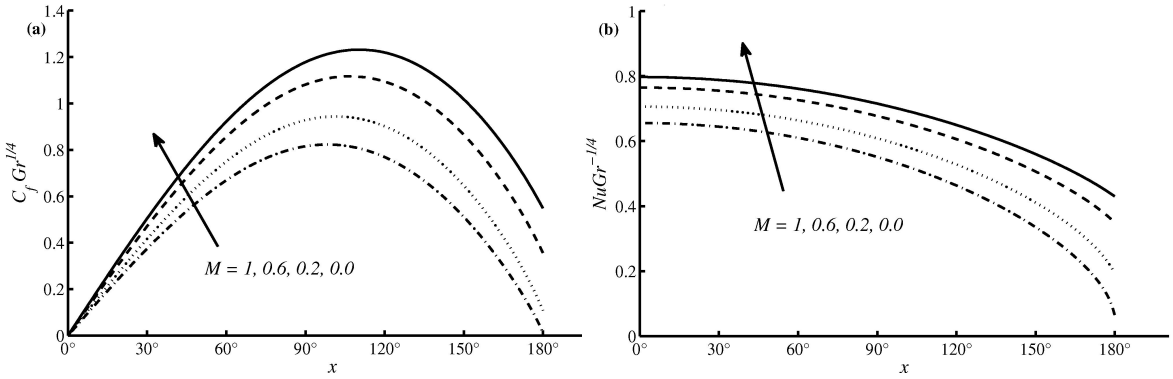

FIGURE 4. (a, b): Variation of $C_f Gr^{1/4}$. and $NuGr^{-1/4}$ for various values of magnetic parameter M while $R_d = 1.5$, Pr = 0.73 and $\theta_w = 1.1$.

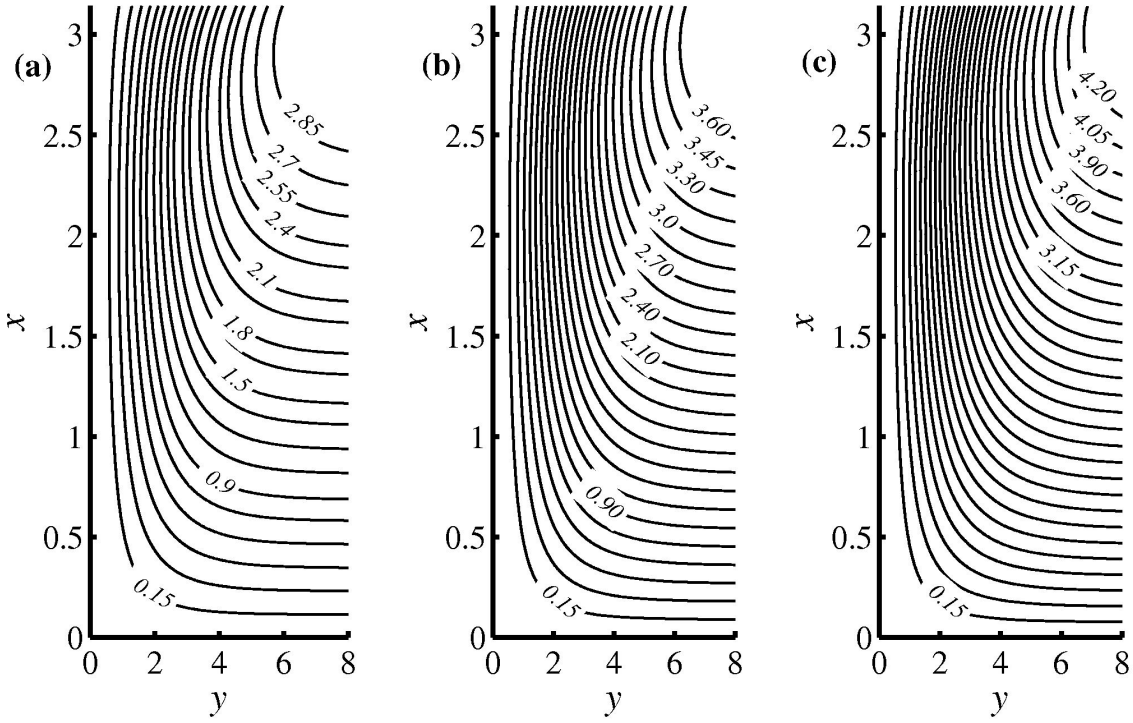

FIGURE 5. (a-c): Streamlines for $R_d = 0$, 0.5, 1.0 respectively while $\theta_w = 1.1$, Pr = 0.73 and $M = 0$.

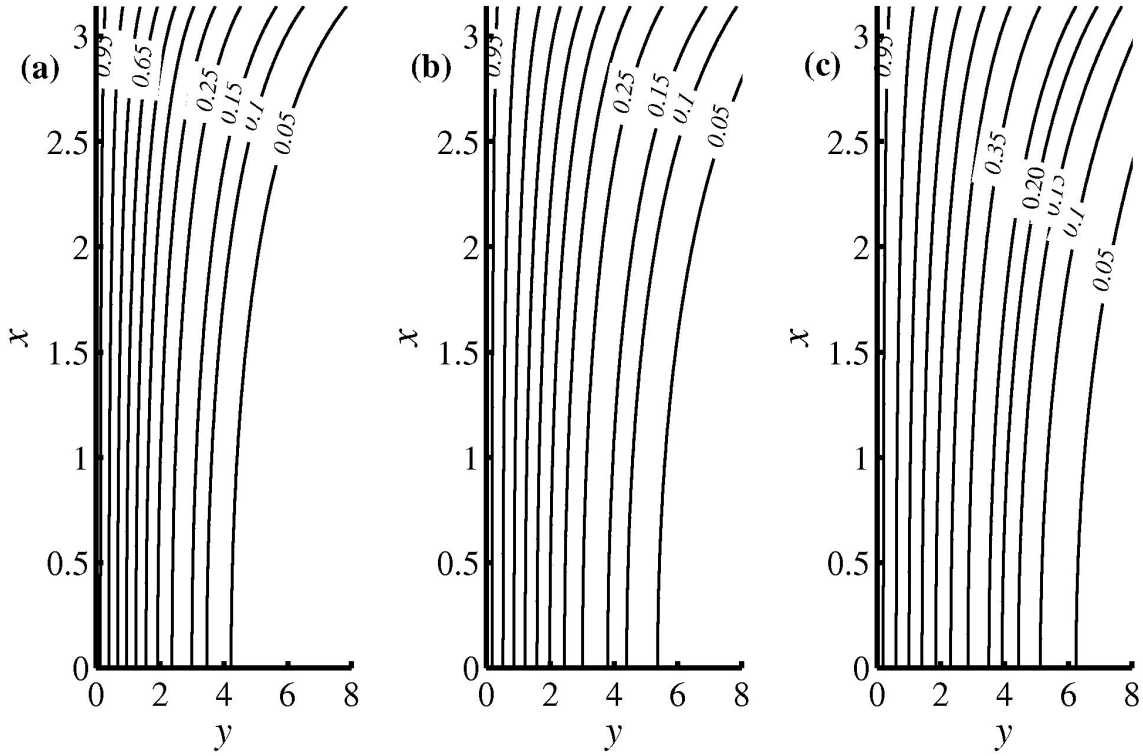

FIGURE 6. (a-c): Isotherms for $R_d = 0.0$, 0.5 and 1.0 respectively while $\theta_w = 1.1$, Pr = 0.73 and $M = 0$.

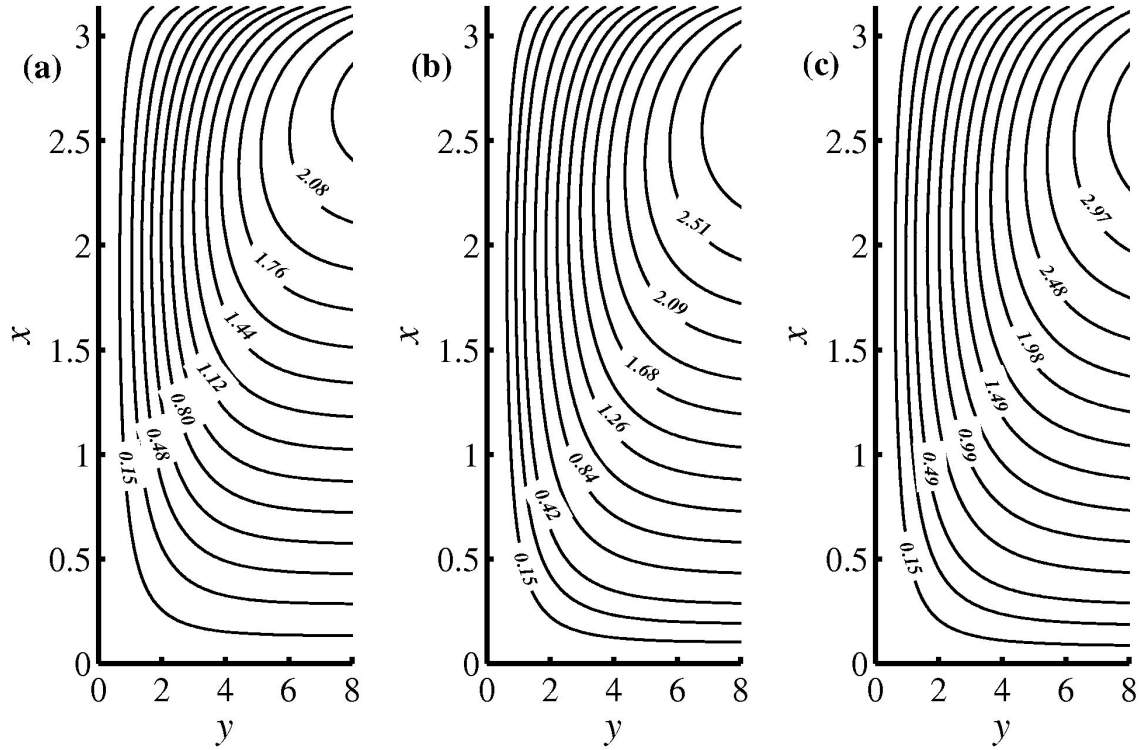

FIGURE 7. (a-c): Streamlines for $R_d = 0.0$, 0.5 and 1.0 respectively while $\theta_w = 1.1$, Pr = 0.73 and $M = 0.5$.

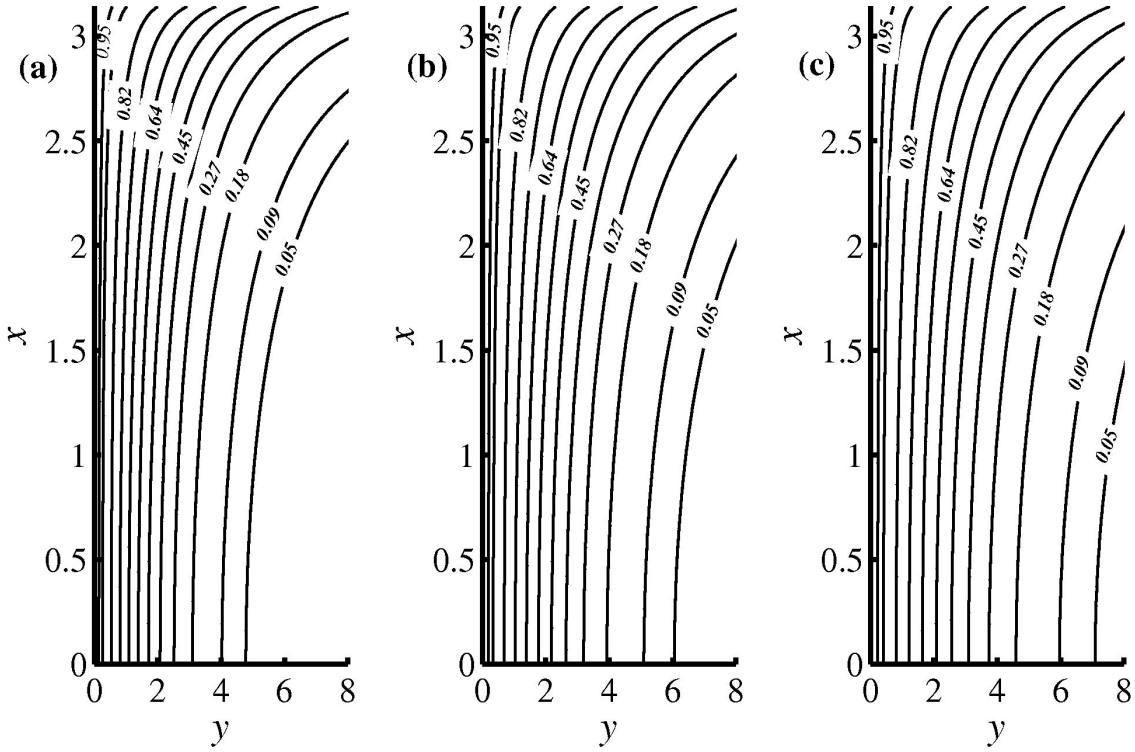

FIGURE 8. (a-c): Isotherms for $R_d = 0.0$, 0.5 and 1.0 respectively $\theta_w = 1.1$, Pr = 0.73 and $M = 0.5$.

ized through Fig. 2(b). Simultaneous effects of magnetic parameter M and R_d on skin-friction coefficient $C_f Gr^{1/4}$ and the Nusselt number $NuGr^{-1/4}$ are plotted in Figs. 3(a, b) respectively. One can see prominent difference between the absence of magnetic parameter ($M = 0.0$) and in the presence of magnetic parameter ($M = 0.5$). As we discussed above magnetic parameter produces resistance in fluid motion and these effects exceeds near the surface of cylinder. So skin friction will decrease in presence of magnetic parameter ($M = 0.5$). It is concluded that skin friction at the surface for $M = 0.0$ remains higher as compare to $M = 0.5$ (Fig. 3(a)). By including the effects of magnetic parameter the thermal energy within boundary layer reduces the temperature difference between surface of cylinder and thermal boundary layer. Hence rate of heat transfer will decrease in presence of magnetic parameter M (Fig. 3(b)). Figs. 4(a, b) show the graphs of $C_f Gr^{1/4}$ (skin friction coefficient) and $NuGr^{-1/4}$ (Nusselt number) for several numeric values of the magnetic parameter M while $R_d = 1.5$, $\theta_w = 1.1$ and Pr = 0.73. These figures depict that by increasing the magnetic parameter M, decrease in the values of $C_f Gr^{1/4}$ and $NuGr^{-1/4}$ is observed. This happens due to the physical fact that the increment in the value of M implies more resistance to momentum and thermal boundary layers. Figures 5(a-c) and 6(a-c) exhibit the growth of streamlines and isotherms in absence of magnetic field ($M = 0$) with fixed values of radiation parameter R_d, which are plotted for Pr = 0.73 and $\theta_w = 1.1$ respectively (related to Molla *et al*. [24]). In presence of magnetic field, it can be seen that without the effect of radiation ($R_d = 0.0$), the value of $\psi_{\max}$ in limited domain is approximately 2.08 analogues to upper stagnation point ($x \approx \pi$) of the cylinder corresponds to the lowest boundary layer thickness and $\psi_{\max}$ slightly increases from 2.08 to 2.97 in Figs. 7(a-c). This rise is not as rapid as seen in Figs. 5(a-c), because magnetic field effect reduces the velocity profile. The isothermal lines for fixed values of R_d with magnetic parameter $M = 0.5$ are shown in Figs. 8(a-c). These isotherms demonstrate that the boundary layer over the surface of the cylinder is grown more prominent as compared to Figs. 6(a-c). The hot fluid attains the maximum height due to gravity with the added effects of magnetic field as x increases from the lower stagnation point ($x \approx 0$), consequently the thickness of the thermal boundary layer increases.

5. Conclusions

We have considered the effect of magnetic field on natural convection boundary layer flow from a circular cylinder in this paper. An implicit finite difference scheme is used to solve the obtained non-dimensional partial differential equations numerically. From the above study, it is observed that by increasing the values of the magnetic parameter M lead to decelerate in velocity and accelerate in temperature distribution. The skin-friction coefficient and Nusselt number are falling down with an increase in magnetic parameter M. The values of the skin friction coefficients and the Nusselt number are rising up with increase values of θ_w. The momentum and thermal boundary layers are decreasing function of magnetic parameter M.

Nomenclature

a	Radius of the circular cylinder	[L]
B_0	applied magnetic field	[kgT^{-2}A^{-1}]
C_f	skin friction coefficient	[-]
c_p	specific heat constant	[L^{2}T^{-2}K^{-1}]
f	dimensionless stream function	[-]
Gr	Grashof number	[-]
g	acceleration due to gravity	[LT^{-2}]
k	thermal conductivity	[kgLT^{-3}K^{-1}]
M	magnetic parameter	[-]
Nu	Nusselt number	[-]
q_w	radiative heat flux	[kgT^{-3}]
R_d	Radiation conduction parameter	
T	fluid temperature in the boundary layer	[K]
T_∞	ambient fluid temperature	[K]
T_w	surface temperature	[K]
u, v	dimensionless velocity components in x and y directions	

Greek symbols

β	thermal expansion coefficient	[K^{-1}]
ρ	fluid density	[kgL^{-3}]
μ	dynamic viscosity	[kgL^{-1}T^{-1}]
σ_0	electric conductivity	[T^{3}A^{2}kg^{-1}K^{-4}]
σ	Stephen- Boltzman constant	[T^{-3}kgK^{-4}]
θ_w	surface heating parameter	[-]
ψ	stream function	[L^{2}T^{-1}]

Subscript

∞	ambient condition	[-]
w	condition at the surface	[-]

1. J.H. Merkin, *Free convection boundary layer on an isothermal horizontal circular cylinders*, ASME/AIChE, Heat Transfer Conference, St. Louis, Mo., U.S.A. (1976) 9-11.
2. J.H. Merkin, *J., Heat Trans.* **99** (1977) 453-57.
3. E.M. Sparrow, and L. Lee, *Int. J. Heat Mass Transf.* **19** (1976) 229-236 .
4. M. Luciano, and De. Socio, *Int. J. Heat Mass Transf.* **26** (1983) 1669-1677.
5. J.H. Merkin, *J. Appl. Maths. Phys*. **29** (1978) 871-883.
6. D.B. Ingham, *Z. Angew Math. Phys.* **29** (1978) 871-883.
7. R. Nazar, N. Amin, and I. Pop, *Heat Transfer*, Proceeding of the Twelfth International Conference, (2002).
8. R. Nazar, N. Amin, and I. Pop, *Int. J. Appl. Mech. Eng.* **7** (2002) 409-431.
9. M.M. Molla, M.A. Hossain, and R.S.R. Gorla, *Heat Mass Transf.* **41** (2005) 594-598.
10. M.M. Molla, M.A. Hossain, and M.C. Paul, *Int. J. Eng. Sci.* **44** (2006) 949-958.
11. M.M. Molla, S.C., Paul, M.A., Hossain, *Appl. Math. Model.* **33** (2009) 3226-3236.
12. S. Bhowmick, M.M. Molla, and M.A. Hossain, *Adv. Mech. Eng.*, (2013) Article ID 194928 doi./10.1155/2013/194928.
13. T. Javed, M.A. Siddiqui, Z. Mehmood, and I. Pop, *Z. Naturforsch* (2015) DOI 10.1515/zna-2015-0232.
14. R.D. Cess, *Int. J. Heat Mass Transf.* **9** (1966) 1269-1277.
15. E.H. Cheng, M.N. Ozisik, *Int. J. Heat Mass Transf.* **15** (1972) 1243-1252.
16. V.S. Arpaci, *Int. J. Heat Mass Transf.* **11** (1968) 871-881.
17. J. Shwartz, *Int. J. Heat Mass Transf.* **1** (1968) 689-697.
18. M.A. Hossain, M.A. Alim, and D.A.S. Rees, *Acta Mech.* **129** (1998) 177-186.
19. M.M. Molla, and M.A. Hossain, *Int. J. Therm. Sci*. **46** (2007) 926-935.
20. K.A. Yih, *Int. J. Heat Mass Transf.* **42** (1999) 4299-4305.
21. T. Akhter, and M.A. Alim, *J. Mech. Eng.* **39** (2008) 50-56.
22. M.M. Molla, M.A. Hossain, and R.S.R. Gorla, *J. Mech. Eng. Sci.* **223** (2009) 1605-1614.
23. M.M. Miraj, M.A. Alim, and M.A.H. Mamun, *Int. Commun. Heat Mass Transf.* **37** (2010) 660-665.
24. M.M. Molla, S.C. Saha, M.A.I. Khan, and M.A. Hossain, *Desalin. Water Treat.* **30** (2011) 89-97.
25. S.M. Mahfooz, M.A. Hossain, R.S.R. Gorla, *Int. J. Therm. Sci.* **58** (2012) 79-91.
26. Z. Abbas, A. Majeed, and T. Javed, *Heat transf. Res.* **44** (2013) 703-718.
27. S. Karthikeyan, M. Bhuvaneswari, S. Rajan, and S. Sivasankaran, *App. Math. Comp. Intel*. **2** (2013) 75-83.
28. S. Siddiqa, M.A. Hossain, S.C. Saha, *Int. J. Therm. Sci.* **84** (2014) 143-150.
29. T. Javed, I. Mustafa, and H. Ahmad, *Therm. Sci.* (2015) doi:10.2298/TSCI140926027J.
30. T. Cebeci, and P. Bradshaw, *Physical and Computational Aspects of Convective Heat Transfer*, (New York, Springer, 1988).
31. Howell, J.R., Siegel, R., and Menguc, M.P., *Thermal Radiation Heat Transfer*, 5th edition, Taylor and Francis, (New York, 2010).